JSS Focus Issue on Semiconductor-Based Sensors

Moisture Insensitive PMMA Coated Pt-AlGaN/GaN Diode Hydrogen Sensor and Its Thermal Stability

Kwang Hyeon Baik,[1] Sunwoo Jung,[2,*] Fan Ren,[3,] S. J. Pearton,[4,**] and Soohwan Jang[2,z]**

[1]*School of Materials Science and Engineering, Hongik University, Jochiwon, Sejong 30016, Korea*
[2]*Department of Chemical Engineering, Dankook University, Yongin 16890, Korea*
[3]*Department of Chemical Engineering, University of Florida, Gainesville, Florida 32611, USA*
[4]*Department of Materials Science and Engineering, University of Florida, Gainesville, Florida 32611, USA*

Poly(methyl methacrylate) (PMMA) encapsulated Pt-AlGaN/GaN Schottky diodes show highly sensitive (100 ppm, 0.01% by volume) room temperature detection of hydrogen and are insensitive to the presence of water in the sensing ambient. These diodes show no physical degradation or loss of sensitivity when repeatedly cycled (50 x, 1 min hold at each temperature) between 25–100°C. There is complete selectivity for hydrogen sensing over other gases, including CO, CO_2, NO_2, O_2 and CH_4. The PMMA encapsulation provides an effective and robust barrier to moisture, greatly increasing the range of environments in which the sensors can be used.

 [DOI: 10.1149/2.002107jss]

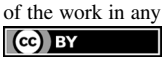

Manuscript submitted January 11, 2018; revised manuscript received February 6, 2018. Published February 16, 2018. *This paper is part of the JSS Focus Issue on Semiconductor-Based Sensors for Application to Vapors, Chemicals, Biological Species, and Medical Diagnosis.*

There is currently great interest in hydrogen as an emission-free fuel for automobiles to both increase fuel economy and decrease vehicle emissions.[1–3] It is expected that hydrogen can become a major energy supply in many applications, including transportation, central and distributed electric power, portable power, and combined heat and power for buildings and industrial processes.[2,3] Since hydrogen gas is extremely reactive with oxygen, and has a low ignition energy, it is prone to spontaneous flammable ignition. It is therefore critically important that robust and fast hydrogen gas detection technologies be available to ensure safe handling.[1–3] In addition, reliable and accurate hydrogen sensor is required in medical diagnosis applications including hydrogen breath test to detect carbohydrate malabsorption and SIBO (small intestinal bacterial overgrowth) of patients.[4–6] Among semiconductor-based hydrogen sensors, various types of wide bandgap GaN (3.4 eV) thin film or nanostructured devices contacted with Pt-or Pd-gate metals are attractive for their robustness and wide operating temperature.[7–21] In particular, the availability of piezoelectric AlGaN/GaN heterostructures enables the design of transistor–based sensors with enhanced sensitivity.[8,9,20,22–24] The AlGaN/GaN high electron mobility transistor (HEMT) structure, with its two dimensional electron gas (2DEG) channel induced by piezoelectric and spontaneous polarization at the interface between the AlGaN and GaN layers, shows highly sensitive current changes to surface charges created by catalytic reaction of hydrogen gas on the Pt or Pd sensing layer. The HEMT based sensor with high carrier density in the 2DEG shows high signal to noise ratio. With 30% Al concentration in the AlGaN layer, 5∼10 times higher channel sheet electron densities are obtained compared to Si, GaAs or InP HEMTs.[25] The AlGaN/GaN heterostructure based Schottky diodes have low concentration detection sensitivities (hundreds of ppm at room temperature), which is well below the concentration at which hydrogen is combustible in the air (4.65%).[3,7,16,17,24] The role of the catalytic metal is to dissociate molecular hydrogen to atomic form, leading to an adsorbed dipole layer at the metal–semiconductor interface.[8,10,15,26–29] This leads to a reduction of the Schottky barrier height, which in turn modulates the current flowing in the device at a fixed operating voltage.[30–32]

The past decade has seen a string of innovations that have increased the detection sensitivities in AlGaN/GaN-based hydrogen sensing, including the (i) use of catalytically active Pt nano-networks on the gate[11–13,23] (ii) surface roughening of the active area using photo-chemical etching to increase the density of available adsorption sites,[10,12,13,16,26] and (iii) using different orientations and surface polarities.[12,14,15,18] In the latter case, it has been observed that semipolar and *c*-plane N-polar GaN have much different responses compared to conventional *c*-plane Ga-face GaN due to the different affinities of hydrogen for the different atomic planes and polarities.[14]

A remaining issue with AlGaN/GaN hydrogen sensors is the fact that their sensitivity is significantly degraded in the presence of humidity or water.[31] This obviously limits their practical application. There are market-driven needs for robust and sensitive sensors to monitor the concentration of hydrogen under humid ambient in the application of hydrogen fuel cell vehicles and hydrogen breath test in medical dioagnosis.[4–6,21,33] Methods to mitigate the effects of absorbed water molecules would be a major step toward expanding these applications. Kumar et al. investigated effects of various polymer encapsulations including poly(methyl methacrylate) (PMMA) on selective hydrogen sensing of nanocrystalline In_2O_3-doped SnO_2 thin film sensors.[21] Yamato et al. reported the mitigation of humidity effect and improved hydrogen sensing characteristics of anodized TiO_2 Schottky diode using polytetrafluoroethylene or polyimide coating.[34] At 25°C, the permeabilities of water and hydrogen in bulk PMMA are 135.1 and 1.15×10^5 mol m^{-1} s^{-1} pa^{-1}, respectively.[35–37] However, the water permeability for PMMA polymer films, which is defined as the product of diffusivity and solubility, dramatically decreases with the thickness of PMMA, and the permeability of thin polymer films is much different from that of the conventional bulk polymer.[38–40] In addition to the permeability, hydrophobicity of the polymer film is also an important factor if it is to be used as a water-blocking layer on hydrogen gas sensors.[21,34] Therefore, a hydrophobic PMMA coating may prevent water molecules from diffusing through the PMMA layer while allowing penetration of hydrogen.

In this paper, we show that encapsulation with poly(methyl methacrylate) (PMMA) provides a robust means of eliminating the sensitivity to moisture of AlGaN/GaN hydrogen sensors. We demonstrate that the encapsulated devices do not suffer from any significant change in hydrogen detection sensitivity in the presence of moisture and that the devices can be repeatedly cycled

*Electrochemical Society Student Member.
**Electrochemical Society Fellow.
[z]E-mail: jangmountain@dankook.ac.kr

to temperatures up to 100°C without any significant change in characteristics.

Experimental

AlGaN/GaN HEMT layer structures were grown on *c*-plane sapphire by metal organic chemical vapor deposition (MOCVD). The epilayer structures were composed of 2 μm thick undoped GaN buffer layer followed by a 35 nm unintentionally doped $Al_{0.3}Ga_{0.7}N$ layer. Sheet resistances of 350 ohm/square, sheet carrier concentrations of 1.06×10^{13} cm^2, and mobilities of 1900 cm^2/Vs were obtained from Hall measurements. ohmic contacts of Ti/Al/Ni/Au were formed by E-beam evaporator and lift-off, and annealed at 850°C for 1 minute under a N_2 ambient. A 200 nm SiN_x layer was deposited for diode isolation by plasma enhanced chemical vapor deposition (PECVD). The windows for active area opening were achieved by buffered oxide etchant (BOE) etching. A 10 nm Pt film was deposited on the diode Schottky contact area by E-beam evaporation. Finally, Ti/Au based contact pads were deposited for probing and wire bonding. For PMMA coating on the device surface, PMMA (Sigma-Aldrich, molecular weight; 996000) was dissolved in anisole with a concentration of 40 mg/mL. 150 nm of PMMA layer was coated on the fabricated device as a moisture barrier after spin-coating at 4000 rpm for 30 s, and removed on the contact areas for probing. The device with PMMA layer was dried in air ambient at 25°C for 1 hour. The thickness of the PMMA layer (150 nm) was chosen to minimize loss of responsivity of hydrogen sensing while maintaining complete coverage of the sensor surface. Figure 1 shows an optical microscope image of the completed devices that included the PMMA encapsulation, along with a schematic of the sensor structure. To test the stability of the encapsulation, devices were cycled 50 times between 25–100°C, with the diodes held for 1 minute at each extreme of this temperature range. Over this temperature range, the PMMA was stable. Current-voltage (I-V) characteristics of both the uncoated and encapsulated Schottky diodes were measured at 25°C using an Agilent 4156C parameter analyzer with the diodes in a gas test chamber in ambients of N_2 or 100–40000 ppm H_2 (corresponding to 0.01–4%) dry hydrogen in nitrogen or the same concentrations of hydrogen bubbled through water to produce 100% relative humidity.

Results and Discussion

Figure 2 shows I-V characteristics of the AlGaN/GaN Schottky diode encapsulated with PMMA before and after 500 ppm dry hydrogen exposure for 30 s. Once hydrogen molecules are exposed to the PMMA encapsulated Pt Schottky diode, they penetrate the PMMA layer and are adsorbed on the catalytic Pt surface. After adsorption on the active sites of Pt, the hydrogen molecules are dissociated into atoms and diffuse to the AlGaN surface, forming dipoles at the interface between Pt and AlGaN.[7,12,16,19,22] This reduces the Schottky barrier height of the diode, resulting in the reduction of turn-on voltage as well as the current increase.

Figure 3a shows time responses of the unencapsulated diode for dry 500 ppm H_2 and 100% relatively humid 500 ppm H_2. Both the dry and wet hydrogen was exposed at a forward bias voltage of 1.3 V for 15 s. The current change of bare devices for humid hydrogen was dramatically reduced, since water molecules blocked the catalytically active Pt sites.[31] By sharp contrast, for PMMA encapsulated devices, the same level of current change was maintained for both dry and wet 500 ppm H_2 exposures as shown in Figure 3b. Hydrophobicity of the polymer film is one of important factors in the water-blocking behavior of PMMA thin film.[21,34] The contact angles of 150 nm PMMA on Pt, and Pt itself, for water were 75° and 8°, respectively. Therefore, the hydrophobic PMMA layer on the Pt Schottky electrode effectively prevented water molecules from diffusing through the PMMA coating while allowing penetration of hydrogen.

Response and recovery times for the unencapsulated and encapsulated Pt-AlGaN/GaN Schottky diode sensors are summarized in Table I. Response time was defined as the time required to reach 90% of peak current after 500 ppm hydrogen exposure for 15 s, and recovery time was defined as the time required to reach 10% of the peak current after refreshing nitrogen exposure. Response times of the bare devices for dry and wet H_2 exposures were 6.8 and 12.5 s, respectively, while response times of the PMMA encapsulated sensors were 8.0 and 11.5 s for dry and humid hydrogen conditions. For both dry and wet hydrogen exposures, the response times of the very thin PMMA-coated devices are similar or longer than those of the bare devices due to the additional time required for in-diffusion through the PMMA layer. The recovery times of the unencapsulated devices were 64.3 and 50.5 s, and those

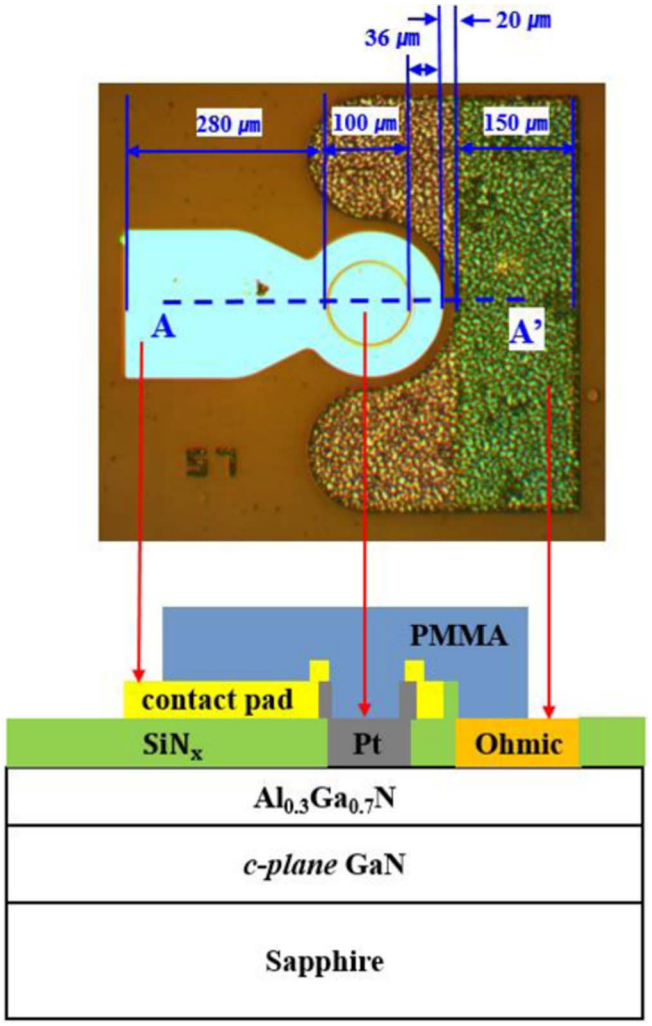

Figure 1. Microscope image and cross-sectional schematic image along the cutline of A-A' of the PMMA encapsulated AlGaN/GaN heterostructure Schottky diode sensor.

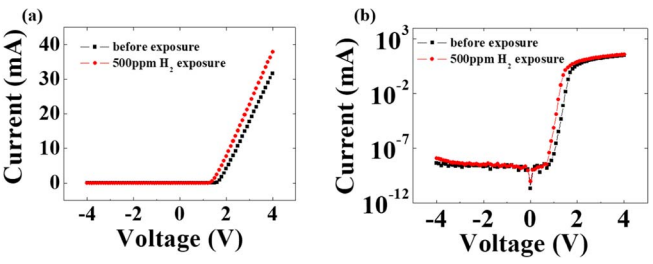

Figure 2. Current-voltage characteristics of PMMA encapsulated diode before and after dry 500 ppm H_2 exposure for 30 s shown on either (a) linear or (b) semi-log scale.

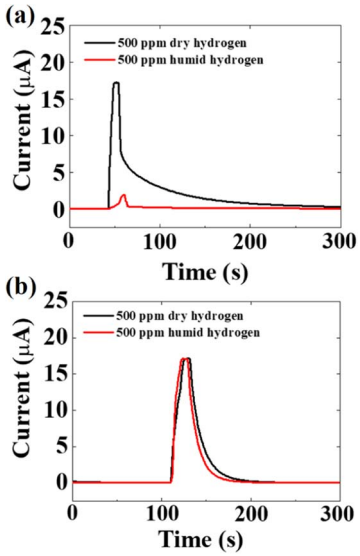

Figure 3. Time response of the forward current at 1.3 V of (a) the unencapsulated and (b) encapsulated diodes for dry 500 ppm hydrogen and 100% relative humid 500 ppm hydrogen exposure for 15 s.

of the PMMA coated devices were 36.0 and 24.8 s, respectively, for dry and humid hydrogen. Water molecules in the ambient are known to enhance out-diffusion of adsorbed hydrogen on Pt due to the larger gradient of hydrogen concentration in Pt.[28] Hence, for both types of devices, shorter recovery times were observed for humid hydrogen compared to dry conditions. Interestingly, the recovery times of the bare devices are longer than those of the PMMA encapsulated sensors for both dry and wet hydrogen exposures. Further work is needed to elucidate detailed sensing mechanisms for the diffusion of hydrogen molecules in the PMMA layer and absorption at the interface between PMMA and Pt.

Figure 4 shows the peak current responses of un-encapsulated and PMMA encapsulated diodes to different concentrations (100–40000 ppm, 0.01–4% by volume) of dry H_2 in N_2. The forward bias voltage was held constant at 1.3 V. The different hydrogen concentrations were introduced for 5 s each and then the test chamber was purged with N_2 prior to introduction of the next hydrogen concentration. The PMMA encapsulated sensor began to respond at a hydrogen concentration of 0.01% or 100 ppm. The response current increases linearly until 2000 ppm concentration of hydrogen, then the increase of the peak current diminishes. The current change upon hydrogen exposure of bare device is slightly larger than that of the encapsulated, but shows similar behavior to the PMMA sensor. The current responses of (b) the bare and (c) PMMA encapsulated diodes to the hydrogen concentration were modeled by using dissociative adsorption Langmuir isotherm:[41,42]

$$I_H = \frac{\alpha(K_{eq} \cdot C)^{\frac{1}{2}}}{1 + (K_{eq} \cdot C)^{\frac{1}{2}}} \quad [1]$$

where I_H is the current change under hydrogen exposure, α is the proportionality constant, K_{eq} is the equilibrium constant of the adsorption, and C is the concentration of hydrogen in ppm. It was assumed that the

Table I. Response and recovery times of the bare and PMMA capsulated sensors for 15 s dry 500 ppm H_2 and 100% relatively humid 500 ppm H_2 exposures.

		Response Time (s)		Recovery Time (s)	
		Average	Standard Deviation	Average	Standard Deviation
unencapsulated Sensor	Dry H_2	6.8	1.5	64.3	28.2
	Wet H_2	12.5	3.5	50.5	27.6
PMMA encapsulated Sensor	Dry H_2	8.0	2.6	36.0	6.4
	Wet H_2	11.5	2.6	24.8	4.3

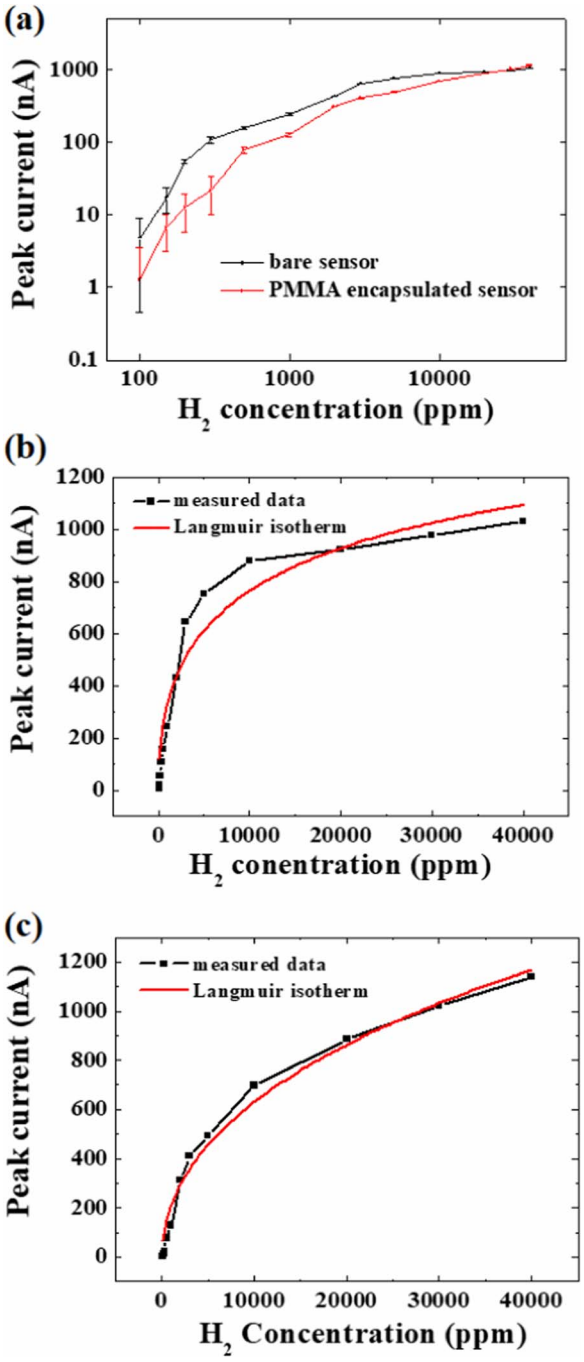

Figure 4. (a) Peak current response of the unencapsulated and encapsulated sensors for a forward bias voltage of 1.3 V as a function of hydrogen concentration over the range of 100–40000 ppm. Each concentration of hydrogen was exposed for 5 s. The same plots were presented in linear scale with Langmuir isotherm models for (b) the bare and (c) the PMMA coated diode. All the samples were measured 5 times for each hydrogen concentration, and the error bars in Figure 4 (a) represent the minimum and maximum values. The medians among the measured data are shown in Figure 4 (b) and (c).

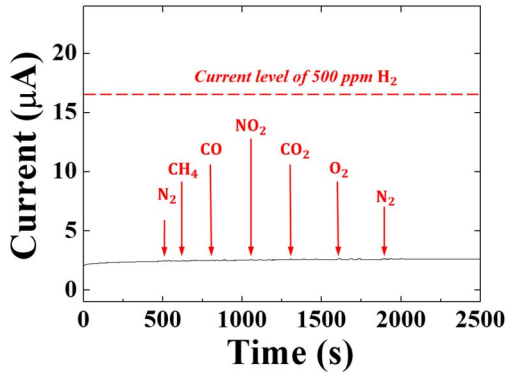

Figure 5. Forward current at 1.3 V forward bias voltage from an encapsulated sensor as different gases are sequentially introduced to the surface (3 cycles of 15 s each for each gas).

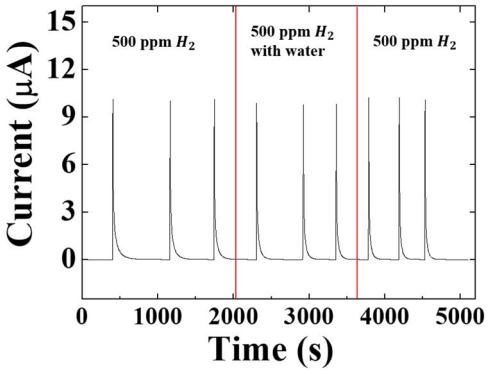

Figure 7. Time response of current at 1.3 V forward bias in encapsulated diodes that had been thermally cycled 50 times from 25–100°C prior to sequential 15 s exposures of 500 ppm of either dry or wet hydrogen.

current change is proportional to the number of hydrogen molecules bound to active sites of Pt surface. It is notable that the power of $\frac{1}{2}$ in the Equation 1 indicates the dissociative adsorption of hydrogen molecules on flat Pt surface and the model matches well the measured data. Hydrogen molecules (after penetrating the thin PMMA layer for the encapsulated diode) are adsorbed on the Pt surface, and then dissociate into hydrogen atoms, resulting in the current increase from the reduction of the Schottky barrier height. The equilibrium constants, K_{eq} were 4.4×10^{-5} and 7.2×10^{-7} for the bare and PMMA coated devices, respectively.

The PMMA encapsulated sensors were completely selective to hydrogen detection, as shown in Figure 5 and did not respond to the other gases we sequentially introduced for three cycles into the test chamber, namely CH_4 (4% in N_2), CO (0.1% in N_2), NO_2 (0.05% in N_2), CO_2 (10% in N_2), and O_2 (100%). Each gas was exposed for 15 s. The concentrations of gases were chosen in the range of U.S. health exposure limits by national institute for occupational safety and health. H_2 molecules (0.298 nm) have the smallest kinetic diameter among those gases including CH_4 (0.380 nm), CO (0.376 nm), NO_2 (0.340 nm), CO_2 (0.330 nm) and O_2 (0.346 nm), hence there exists the most possibility for H_2 to penetrate the PMMA layer.[43] The small transients upon introduction of each gas are due to the pressure variations at the surface of the sensor as each gas is directed toward it.

The diode encapsulated with PMMA whose glass transition temperature is 105°C[44] was thermally cycled from 25°C to 100°C to check the thermal stability of the device. The sensor was kept at 25°C and 100°C for 1 minute each in an air ambient, and this process was repeated 50 times. Sensitivities of the PMMA encapsulated sensor as a function of bias voltage before and after 50 times heat cycles are shown in Figure 6. The sensitivity is defined as $\frac{I_H - I_N}{I_N} \times 100\%$, where

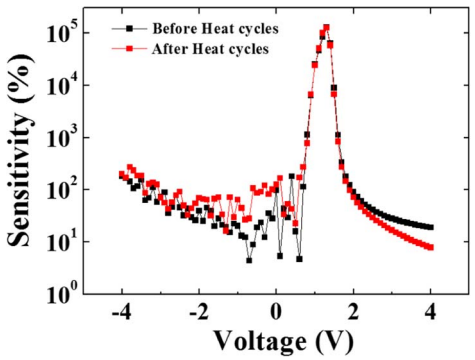

Figure 6. Sensitivities as a function of bias voltage before and after 50 heat cycles over the range of 25–100°C. The device was kept for 1 min. at each extreme temperature. Exposure to the 500 ppm hydrogen was for 30 s in each case.

I_H is the current under dry 500 ppm H_2 and I_N is the current under N_2. The PMMA sensors show a maximum sensitivity of 1.2×10^5 at 1.3 V (which is the turn-on voltage of the diode shown in Figure 2) before the thermal stress. The heat cycled device does not show any change in maximum sensitivity and the corresponding bias. Also, the same level of sensitivity was maintained between 0.5 and 2 V after 50 times heat cycles.

As we noted earlier, the presence of humidity decreases the hydrogen detection sensitivity of unencapsulated Pt-AlGaN/GaN diodes. At 500 ppm, this amounts to a decrease of about a factor of 8 in absolute current response for 100% humidity level (Figure 3). By sharp contrast, the PMMA encapsulated diodes do not show this decrease in sensitivity and moreover, the thermally cycled sensors retain their imperviousness to humidity. Figure 7 shows the time response of current in encapsulated diodes that had been thermally cycled 50 times from 25 to 100°C and then cyclically exposed to dry and wet H_2. Three cycles of dry 500 ppm H_2, followed by switching to wet H_2 for 3 cycles and then back to the dry H_2 were imposed on the device. The wet hydrogen was obtained by bubbling the hydrogen through two bubblers of water to create a 100% relative humidity level. There was no difference in response of the sensors in the presence of 100% relative humidity, and no significant degradation was found after thermal cycling. This also confirms that the PMMA is a very effective and stable moisture barrier under 100°C and prevents blocking of hydrogen adsorption sites on the Pt by water molecules, which is thought to be the mechanism for the decrease in sensitivity of these hydrogen sensors in the presence of humidity.[31]

Conclusions

Unencapsulated Pt-AlGaN/GaN diode sensors suffer a major decrease in sensitivity in the presence of the water vapor content in the hydrogen.[31] The use of PMMA encapsulation is completely successful in eliminating this decrease due to the increased humidity level, while still retaining the same absolute detection sensitivity ($\sim 2.8 \times 10^5$% at low forward bias voltage). Other common polymers such as poly(vinyl chloride), poly(ethylene) and poly(trifluoro chloroethylene) have even lower permeability coefficients for moisture and could also be used for hydrogen sensor encapsulation.[35] Our results show that the PMMA can be repeatedly thermally cycled between room temperature and 100°C without any degradation of moisture barrier properties on the Pt-AlGaN/GaN hydrogen sensors. This is an effective solution to deploying the sensors in ambients in which the humidity is likely to vary with time.

Acknowledgments

This research was supported by the Basic Science Research Program through the National Research Foundation of Korea (NRF)

funded by the Ministry of Education (2015R1D1A1A01058663, 2017R1D1A3B03035420), and Nano Material Technology Development Program through the National Research Foundation of Korea (NRF) funded by the Ministry of Science, ICT and Future Planning (2015M3A7B7045185). The work at UF was partially supported by HDTRA1-17-1-0011.

ORCID

Fan Ren https://orcid.org/0000-0001-9234-019X
S. J. Pearton https://orcid.org/0000-0001-6498-1256
Soohwan Jang https://orcid.org/0000-0002-8188-6274

References

1. J. Kim and I. Moon, *Int. J. Hydrogen Energy*, **33**, 5887 (2008).
2. G. R. Astbury and S. J. Hawksworth, *Int. J. Hydrogen Energy*, **32**, 2178 (2007).
3. T. Hübert, L. Boon-Brett, V. Palmisano, and M. A. Bader, *Int. J. Hydrogen Energy*, **39**, 20474 (2014).
4. C. J. Böhmer and H. A. Tuynman, *Eur. J. Gastroenterol. Hepatol.*, **8**, 1013 (1996).
5. M. Pimentel, E. J. Chow, and H. C. Lin, *Am. J. Gastroenterol.*, **95**, 3503 (2000).
6. M. Pimentel, E. J. Chow, and H. C. Lin, *Am. J. Gastroenterol.*, **98**, 412 (2003).
7. J. Song, W. Lu, J. S. Flynn, and G. R. Brandes, *Solid-State Electron.*, **49**, 1330 (2005).
8. H. Wang, T. J. Anderson, F. Ren, C. Li, Z. Low, J. Lin, B. P. Gila, S. J. Pearton, A. Osinsky, and A. Dabiran, *Appl. Phys. Lett.*, **89**, 242111 (2006).
9. H. T. Wang, B. S. Kang, F. Ren, L. C. Tien, P. W. Sadik, D. P. Norton, S. J. Pearton, and J. Lin, *Appl. Phys. Lett.*, **86**, 243503 (2005).
10. S. Jang, J. Kim, and K. H. Baik, *J. Electrochem. Soc.*, **163**, B456 (2016).
11. K. H. Baik, J. Kim, and S. Jang, *ECS Trans.*, **72**, 23 (2016).
12. S. Jang, P. Son, J. Kim, S. Lee, and K. H. Baik, *Sens. Actuators, B*, **222**, 43 (2016).
13. H. Kim, K. H. Baik, F. Ren, S. J. Pearton, and S. Jang, *ECS Trans.*, **61**, 353 (2014).
14. K. H. Baik, H. Kim, S. Lee, E. Lim, S. J. Pearton, F. Ren, and S. Jang, *Appl. Phys. Lett.*, **104**, 072103 (2014).
15. H. Kim, W. Lim, J. Lee, S. J. Pearton, F. Ren, and S. Jang, *Sens. Actuators, B*, **164**, 64 (2012).
16. K. Matsuo, N. Negoro, J. Kotani, T. Hashizume, and H. Hasegawa, *Appl. Surf. Sci.*, **244**, 273 (2005).
17. A. Zhong, T. Sasaki, and K. Hane, *Sens. Actuators A*, **209**, 52 (2014).
18. H. Kim and S. Jang, *Curr. Appl. Phys.*, **13**, 1746 (2013).
19. J. Song, W. Lu, J. S. Flynn, and G. R. Brandes, *Appl. Phys. Lett.*, **87**, 133501 (2005).
20. W. Lim, J. S. Wright, B. P. Gila, J. L. Johnson, A. Ural, T. Anderson, F. Ren, and S. J. Pearton, *Appl. Phys. Lett.*, **93**, 72109 (2008).
21. A. Kumar, P. Zhang, A. Vincent, R. McCormack, R. Kalyanaraman, H. J. Cho, and S. Seal, *Sensors and Actuators B*, **155**, 884 (2011).
22. T. J. Anderson, H. T. Wang, B. S. Kang, F. Ren, S. J. Pearton, A. Osinsky, A. Dabiran, and P. P. Chow, *Appl. Surf. Sci.*, **255**, 2524 (2008).
23. C. Chen, H. Chen, I. Liu, H. Liu, P. Chou, J. Liou, and W. Liu, *Sens. Actuators B*, **211**, 303 (2015).
24. X. Yu, C. Li, Z. N. Low, J. Lin, T. J. Anderson, H. T. Wang, F. Ren, Y. L. Wang, C. Y. Chang, S. J. Pearton, C. H. Hsu, A. Osinsky, A. Dabiran, P. Chow, C. Balaban, and J. Painter, *Sens. Actuators B*, **135**, 188 (2008).
25. S. Jung, K. H. Baik, F. Ren, S. J. Pearton, and S. Jang, *J. Electrochem. Soc.*, **164**, B417 (2017).
26. K. H. Baik, J. Kim, and S. Jang, *Sens. Actuators B*, **238**, 462 (2017).
27. A. Zhong, T. Sasaki, and K. Hane, *Int. J. Hydrogen Energy*, **39**, 8564 (2014).
28. Y. Tsai, K. Lin, H. Chen, I. Liu, C. Hung, T. Chen, T. Tsai, L. Chen, K. Chu, and W. Liu, *J. Appl. Phys.*, **104**, 024515 (2008).
29. Y. Irokawa, *J. Appl. Phys.*, **113**, 026104 (2013).
30. C. Lo, S. Tan, C. Wei, J. Tsai, K. Hsu, and W. Lour, *Int. J. Hydrogen Energy*, **37**, 18579 (2012).
31. C. F. Lo, C. Y. Chang, B. H. Chu, S. J. Pearton, A. Dabiran, P. P. Chow, and F. Ren, *Appl. Phys. Lett.*, **96**, 232106 (2010).
32. B. S. Kang, S. Kim, F. Ren, B. P. Gila, C. R. Abernathy, and S. J. Pearton, *Sens. Actuators, B*, **104**, 232 (2005).
33. A. Bazylak, *Int. J. Hydrogen Energy*, **34**, 3845 (2009)
34. G. Yamamoto, T. Yamashita, K. Matsuo, T. Hyodo, and Y. Shimizu, *Sens. Actuators B*, **183**, 253 (2013).
35. R. J. Ashley, *Permeability and Plastics Packaging in Polymer Permeability*, edited by J. Comyn, Elsevier Applied Science Publishers, London, (1985) 269
36. K. J. Jeon, H. R. Moon, A. M. Ruminski, B. Jiang, C. Kisielowski, R. Bardhan, and J. J. Urban, *Nature Materials*, **10**, 286 (2011).
37. J. Gao, B. Li, J. Tan, P. Chow, T.-M. Lu, and N. Koratkar, *ACS Nano*, **10**, 2628 (2016).
38. C. L. Soles, J. F. Douglas, and W. L. Wu, *J. Polym. Sci. B*, **42**, 3218 (2004).
39. B. D. Voigt, C. I. Soles, H. Lee, E. K. Lin, and W. Wu, *Langmuir*, **20**, 1453 (2004).
40. A. Sundaramoorthi, *Fundamental understanding of physicochemical properties of ultra-thin polymer films*, (Ph. D thesis), Georgia institute of technology, 2011.
41. G. Lee, S. Kim, S. Jung, S. Jang, and J. Kim, *Sens. Actuators B*, **250**, 569 (2017).
42. C. Wen, Q. Ye, S.-L. Zhang, and D. Wu, *Sens. Actuators B*, **223**, 791 (2016).
43. J. Hong, S. Lee, J. Seo, S. Pyo, J. Kim, and T. Lee, *ACS Appl. Mater. Interfaces*, **7**, 3554 (2015).
44. S. Y. Chou, P. R. Krauss, and P. J. Renstrom, *Appl. Phys. Lett.*, **67**, 3114 (1995).